J Solid State Electrochem (2009) 13:171–179
DOI 10.1007/s10008-008-0614-3

ORIGINAL PAPER

Chronopotentiometric method for the assessment of ionophore diffusion coefficients in solvent polymeric membranes

Sándor Bodor · Justin M. Zook · Ernő Lindner · Klára Tóth · Róbert E. Gyurcsányi

Received: 7 May 2008 / Revised: 10 June 2008 / Accepted: 11 June 2008 / Published online: 16 July 2008

Abstract A chronopotentiometric method is proposed for the determination of the diffusion coefficients of free ionophores in solvent polymeric membranes. For the pH sensitive chromoionophore ETH 5294, the method was shown to give diffusion coefficients that correlate well with those assessed by both optical and chronoamperometric methods. The limit of applicability of the chronoamperometric and chronopotentiometric methods in terms of membrane composition and experimental parameters has been identified. The chronopotentiometric method was successfully used to determine the diffusion coefficients of eight ionophores and proved to be more robust and more widely applicable than the previously reported chronoamperometric and optical methods.

Keywords Ion-selective electrode · Silver · Sodium · Calcium · Potassium · Lead ionophore · Diffusion coefficient · Plasticized PVC membranes · Chronopotentiometry

S. Bodor · K. Tóth · R. E. Gyurcsányi (✉)
Department of Inorganic and Analytical Chemistry,
Budapest University of Technology and Economics,
Szt. Gellért tér 4,
Budapest 1111, Hungary
e-mail: robertgy@mail.bme.hu

K. Tóth · R. E. Gyurcsányi
Research Group of Technical Analytical Chemistry
of the Hungarian Academy of Sciences,
Budapest University of Technology and Economics,
Szt. Gellért tér 4,
Budapest 1111, Hungary

J. M. Zook · E. Lindner
Department of Biomedical Engineering,
The University of Memphis,
Memphis, TN 38152, USA

Introduction

Ion-selective electrodes (ISEs) have become established routine analytical tools. In the last 10 years, the interest for ionophore-based ISEs increased spectacularly due to the extension of their detection limits to concentrations as low as 10^{-12} M [1]. In these sensors, the control of transmembrane ion fluxes and concomitant ion concentration changes at the two membrane/solution interfaces are of primary importance [2–6]. Transmembrane fluxes are important because they can lead to the contamination of the solution layer in the vicinity of the sensing membrane [7], and by that adversely affect the selectivity coefficients and detection limit of the respective ISEs [8]. Improved detection limits are achieved by minimizing the contamination, which translates into an accurate control of the ion transport across the membrane. In general, the primary ion flux across an ion selective membrane is controlled by establishing a concentration [1, 2, 9] and/or an electric field gradient across the membrane [10, 11]. Alternative methods to minimize the contamination at the sensing surface of an ISE utilize increased mass transport in the sample solution [4, 6], in combination with low diffusivity membranes [12, 13] and elaborate conditioning procedures [14, 15]. Consequently, the knowledge of the diffusion coefficients of the active components in the membrane is a prerequisite for the rational design of ISEs with improved performance characteristics. This knowledge gained additional importance with the miniaturization of ionophore based ISEs [16] and optodes [17] because they have extremely small volumes of membranes in which the ionophore content is in the range of femtomoles [16] or lower, even for relatively high ionophore concentrations (10^{-3}–10^{-2} M). The loss of ionophore from the IS membrane deteriorates the response of the sensors and limits their lifetime. There is a strong

correlation between diffusion coefficients of active components in the membrane matrix and the lifetime of the sensors [18].

Recently there has been an increased interest in switching ISEs from passive to active probes. It has been shown that an externally applied current or potential, can lead to improved detection limits [6, 10], increased sensitivity [19], and better selectivity coefficients [6, 10, 20]. In addition, with the advent of current polarized membranes new applications emerged, e.g., selective coulometric release of ions for titration [21]. In all of these new sensing schemes and sensors the diffusion/migration controlled mass transport of ions, ionophores, and lipophilic additives [22–28] has fundamental importance, i.e., the knowledge of their mobility in the IS membrane is essential.

With the increasing importance of mass transport controlled ISEs, the methods available for the determination of the diffusion coefficients of ionophores in solvent polymeric membranes [29, 30] have been recently complemented with a series of new methods. In the "merged membrane" method of Püntener et al. [31], the diffusion coefficients are determined by fitting theoretical diffusion equations [32] to the concentration profiles of chromoionophores recorded optically, perpendicular to the interface between an ionophore loaded and a blank membrane. This method and its extensions [33, 34] are, however, only applicable to chromoionophores, i.e., ionophores with light absorption in the visible range. To overcome this limitation we implemented a chronoamperometric (CA) method for the determination of the diffusion coefficients, which was validated for ETH 5294 pH sensitive chromoionophore using established optical methods [35]. The results provided by the two methods were in excellent agreement despite the differences in the experimental conditions: the optical measurements employ dry membranes, while in the CA experiments membranes conditioned in aqueous solution are used.

The CA method utilizes a characteristic breakpoint in the current–time transients for the determination of the diffusion coefficient of free ionophores. The time instance corresponding to the breakpoint, τ, is a function of the diffusion coefficient of the ionophore as shown in Eq. 1:

$$\tau^{1/2} = \frac{FARC_{\mathrm{L,free}}\sqrt{D_{\mathrm{L,free}}\pi}}{2V} = \frac{FAC_{\mathrm{L,free}}\sqrt{D_{\mathrm{L,free}}\pi}}{2I_{\mathrm{init}}} \qquad (1)$$

where A is the area of the membrane exposed to the solution, R is the bulk membrane resistance, V is the applied voltage, $I_{\mathrm{init}}=V/R$ is the initial current, $C_{\mathrm{L,free}}$ and $D_{\mathrm{L,free}}$ are the concentration and diffusion coefficient of the free ionophore, respectively. However, for estimating the ionic fluxes in mass transport controlled ISEs, not the free ionophore, but the ion–ionophore complex diffusion coefficient is the most pertinent. The ion–ionophore complex diffusion coefficient [7] can be determined in potentiometric ion breakthrough experiments. As we have shown recently [35] the diffusion coefficients for higher stoichiometry complexes can be significantly different from that of the free ionophores, e.g., in the case of ETH 5234 Ca^{2+}-selective ionophore, which forms a 3:1 stoichiometry complex with Ca^{2+}. However, the diffusion coefficients of the free and complexed ionophore can be converted into each other by inserting their corrected molecular radius into the Einstein–Stokes equation [35]. Although the use of the Einstein–Stokes equation in solvent polymeric membranes is subject to limitations, we found excellent agreement between the experimentally determined diffusion coefficients and those calculated from the molecular geometry [35].

Unfortunately the chronoamperometric method has certain inherent uncertainties related to the constant current assumption before the breakpoint [22, 23]. This assumption is valid primarily for fixed site membranes [36], while mobile site membranes show a decrease in the measured current before the breakpoint [37]. Recently, it has been shown that Eq. 1 applies also for galvanostatic polarization, i.e., for the assessment of the diffusion coefficients from chronopotentiometric (CP) experiments [22–27]. The only difference is that in CP experiments the applied constant current is inserted into Eq. 1 instead of the ratio of the applied voltage and bulk membrane resistance. Consequently, the uncertainties due to changing membrane resistance in CA measurements, i.e., varying current before the occurrence of the breakpoint, can be eliminated in CP experiments. These advantages motivated the present work in which the diffusion coefficients of eight cation-selective ionophores (Fig. 1) were determined by using the chronopotentiometric method. The selected ionophores are among the most often used molecules in the practice of ISEs. Some of them were utilized for the fabrication of ISEs for ultra-trace analysis [9, 38]. The uncertainties associated with the chronoamperometric determinations are provided and the applicability criteria of both CA and CP methods are discussed.

Experimental

Chemicals and reagents

Selectophore grade poly(vinyl chloride) (PVC), bis(2-ethylhexyl) sebacate (DOS), ortho-nitrophenyloctylether (o-NPOE), sodium tetrakis[3,5-bis(trifluoromethyl)phenyl]borate (NaTFPB), Calcium ionophore IV: N,N-dicyclohexyl-N', N''-dioctadecyl-3-oxapentanediamide (ETH 5234) [39],

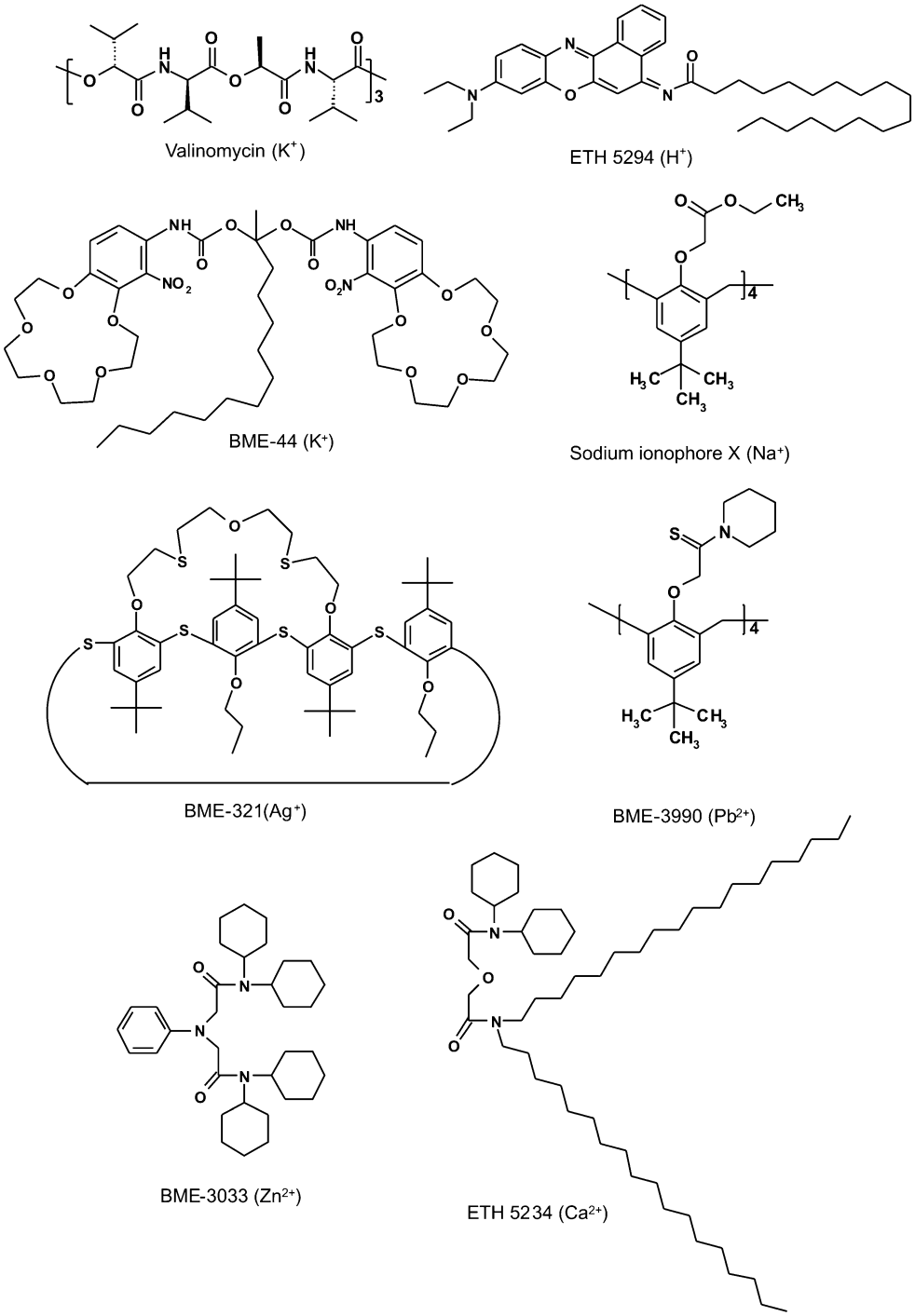

Fig. 1 Chemical structures of the ionophores involved in the present study

Valinomycin, Potassium ionophore III: 2-Dodecyl-2-methyl-1, 3-propanediylbis[*N*-[5'-nitro(benzo-15-crown-5)-4'-yl] carbamate] (BME-44) [40], Sodium ionophore X: (4-*tert*-Butylcalix[4]arene-tetraacetic acid tetraethyl ester) [41] and tetrahydrofuran (THF) were from Fluka (Buchs, Switzerland). The silver, 1,3-*alt*-5,11,17,23-tetra-*tert*-butyl-25, 27-dipropoxy-26,28-(3,9-dithia-6-oxaundec-1,11-diyloxy)thia-calix[4]arene (BME-321) [9, 42], lead, 5,11,17,23-tetra-*tert*-butyl-25,26,27,28-tetrakis-(piperidinothiocarbo-nylmethoxy) calix[4]arene (BME-3990), and zinc, *N*-Phenyl-iminodiacetic acid *N′*-*N″*-dicyclohexyl-*bis*-amide (BME-3033)[43], ionophores were synthesized by the Department of Organic Chemistry and Technology, Budapest University of Technology and Economics. Suprapur® grade sodium chloride, calcium chloride tetrahydrate were obtained from Merck (Darmstadt, Germany). All other salts were of analytical grade and were purchased from Fluka. Solutions were prepared using deionized water with a resistivity of 18.2 MΩ × cm (Millipore, Synergy Water Purification System, Molsheim, France).

Membranes

Membrane components were dissolved in 2 ml THF and cast in 27 mm diameter glass rings. The compositions of the membranes used in the present study are listed in Table 1.

Experimental setup

The chronoamperometric and chronopotentiometric experiments were performed in custom-made electrochemical transport cells [35] in which the IS membrane with an effective surface area of 0.785 cm^2, separated two 20 mL volume compartments. Each compartment accommodated an embedded, disk-shaped Ag/AgCl electrode (ϕ=0.75 cm) connected to an Autolab Pgstat 12 potentiostat/galvanostat (Eco Chemie B.V., Utrecht, The Netherlands). The CA and CP experiments were performed in a symmetrical setup, i.e. with solutions of the same composition on both sides of the membranes. Before the experiments, the membranes were equilibrated for at least 1 day in these solutions. One millimolar solutions of the primary ions were used as bathing solutions except for H^+- and Ag^+-selective membranes where 50mM citrate buffer (pH=5.00) and 10^{-3} M $AgNO_3$ in 10^{-2} M $NaNO_3$ were used, respectively. In CA experiments the membrane potential was recorded in stirred solutions before and after the application of the external voltage. The selection of the applied voltage in CA experiments (or the applied current in CP experiments) is an important consideration. The breakpoints in the transients are most pronounced when the initial current is much larger than the final limiting current. Since the initial ohmic current is proportional to the applied voltage but the final limiting current is not, larger applied voltages make the breakpoints in the CA transients more pronounced. However, too large applied voltages can lead to the breakdown of the membrane permselectivity (Donnan exclusion failure). On the other hand, low applied voltages result in larger τ values, which are concomitant to smaller relative errors in the experimentally determined breakpoint times. But the overall signal changes are smaller and the breakpoints are blurred when the CA experiments are performed with relatively low applied voltages. [35, 36] (see eq. 19 in

Table 1 The composition of the ion-selective membranes used in this study

Membrane	PVC	DOS	ONPOE	Ionophore		NaTFPB			Resistance (kΩ)	
	mg	mg	mg	mg	mM	Mg	mM	mol%	Membrane[a]	Solution[b]
Ca-DOS-25	49.77	149.29		1.681	10.72	0.889	5.13	47.8	260	16
Ca-DOS-33	66.48	132.81		1.685	11.15	0.89	5.32	47.8	513	16
Ca-DOS-40	79.44	119.72		1.58	10.76	0.89	5.48	50.9	827	16
Ca-DOS-48	95.15	103.22		1.686	11.94	0.889	5.69	47.7	1989	16
Ca-oNPOE-25	49.8		150.34	0.339	2.38	0.177	1.13	47.2	39	16
Ca-oNPOE-33	66.32		132.73	0.328	2.43	0.178	1.16	47.6	99	16
Ca-oNPOE-40	79.62		119.24	0.336	2.48	0.179	1.2	48.2	196	16
Ca-oNPOE-48	95.37		103.55	0.34	2.55	0.18	1.22	47.9	607	16
Ca-oNPOE-55	109.38		89.29	1.687	12.87	0.886	6.11	47.5	272	16
H-DOS-25	49.8	149.16		1.229	10.78	0.89	5.14	47.7	48	0.382
H-DOS-33	66.26	132.47		1.224	11.17	0.886	5.33	47.7	69	0.382
H-DOS-45	89.44	109.23		1.224	11.69	0.887	5.58	47.8	201	0.382
H-DOS-55	109.33	89.57		1.223	12.19	0.885	5.81	47.7	469	0.382
H-oNPOE-25	49.89		148.69	1.229	11.85	0.889	5.65	47.7	7	0.382
H-oNPOE-33	66.25		132.12	1.227	12.05	0.884	5.72	47.5	16	0.382
H-oNPOE-45	89.35		109.2	1.228	12.47	0.889	5.95	47.7	49	0.382
H-oNPOE-55	109.4		89.72	1.23	12.88	0.889	6.13	47.6	214	0.382
K-Val-DOS-33	66.71	133.84		0.779	3.72	0.448	2.68	72.3	347	26
Ag-DOS-33	66.20	132.30		0.703	3.78	0.440	2.66	70.5	260[c]	6[c]
K-BME-DOS-33	66.54	132.97		0.672	3.71	0.440	2.65	71.7	324	26
Na-DOS-33	66.51	132.54		0.704	3.79	0.444	2.68	70.6	249	31
Pb-DOS-33	66.45	133.05		0.493	2.17	0.538	3.20	147.3	718	17
Zn-DOS-33	66.78	133.42		0.379	3.77	0.448	2.69	71.5	780	17

[a] The bulk resistance of the fully conditioned membranes was determined in similar conditions, however, with the respective IS membrane separating the two compartments. In case of ETH 5294 pH sensitive membranes a 50 mM citrate buffer (pH=5.00) (containing 0.055 M Cl^-) was used as bathing solution. [c] The bathing solution was 10^{-3} M $AgNO_3$ in 10^{-2} M $NaNO_3$

[b] The bulk resistaces of the fully conditioned membranes were determined in the same solutions and transport cell as utilized in the CA and CP studies

ref. [37]). Blurred breakpoints are associated with larger standard deviations in the experimentally determined breakpoint times. Consequently, the selection of the adequate voltage, in CA experiments, or current, in CP experiments, is a compromise between these two opposite effects. In practice the values of the applied voltage or current are selected to have breakpoint times between 20–100 s. Preceding the application of a constant voltage or current, the bulk resistance of the membrane was determined by impedance spectroscopy (E_{appl}=0 V; voltage amplitude, 5 mV; frequency range, 1–100 kHz). This measured resistance was used to select, based on Eqs. 2 and 3, the adequate voltage (1–5 V) or current values (1–7 μA) for transients with clear, reproducible breakpoints. This approach worked well with most of the membrane compositions, but the evaluation of the breakpoints remained challenging with certain membrane formulations (Fig. 2b).

The CA and CP experiments were performed in stirred solutions while the transmembrane current or the membrane potential has been continuously monitored, respectively. All the diffusion coefficients reported are average of three successive measurements, each performed at a different applied voltage or current within the previously determined optimal range.

Results and discussions

Early studies involving externally applied voltages were aimed to understand the permselectivity and the mechanism of ion transport in neutral ionophore-based cation-selective membranes [44, 45]. These studies revealed that upon the application of adequately large voltages across the membranes the resulting current–time curves exhibit certain breakpoints, dividing the transients into two regions with largely dissimilar slopes [45]. Morf has explained the ion transport process as being a "closed loop" mechanism [46, 47], in which the current is controlled by the ion up-take and release rate at the opposite sides of the membrane that is coupled with the back diffusion of the free ionophore. Thus the voltage induced ion transport through the membrane tilts the concentration profiles of the ionophore, ionophore–ion complex, and mobile anionic sites in the membrane cross-section. If the applied voltage is sufficiently large, the depletion of the free ionophore at the positive side of the membrane cannot be compensated by the back diffusion, consequently its concentration approaches zero at the interface [24–26]. The depletion of the free ionophore at the positive side of the membrane impedes the cation uptake and triggers an increase in the transmembrane resistance which leads to a rapid drop in the current. Accordingly, breakpoints in the current–time transients are in fact due to the consumption of the free ionophore at the positive side of the membrane (where the cations enter). As shown in Eq. 1, the breakpoint time (τ) in CA experiments depends on the applied voltage, the concentration of the free ionophore and its diffusion coefficient in the membrane [37].

A more general form of Eq. 1 has been introduced in our previous work that considers the ion–ionophore complex stoichiometry (k) and the charge (n) of the primary ion, while it assumes a single negative charge for the mobile anionic sites in the membrane [35]:

$$\tau^{1/2} = \frac{nFA\left(C_{L,tot} - \frac{k}{n}C_{site}\right)\sqrt{D_{L,free}\,\pi}}{2\,k\,I_{init}} \qquad (2)$$

where, $D_{L,free}$ is the diffusion coefficient of the free ionophore, A is the area of the membrane in contact with the solution, F is the Faraday number, $C_{L,tot}$ and C_{site} are the total concentrations of the ionophore and of the lipophilic anion added to the membrane, respectively. The

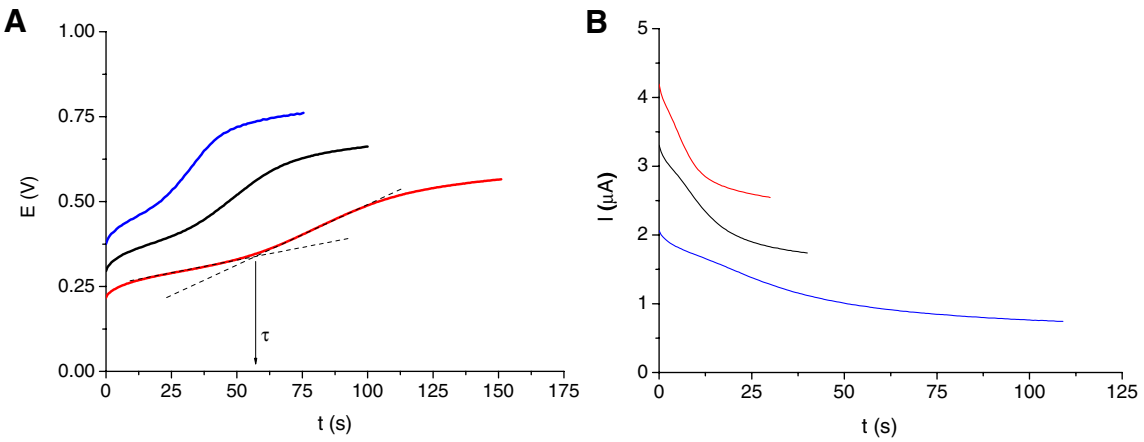

Fig. 2 Comparison of the chronopotentiometric (**a**) (I_{appl}=1, 1.25 and 1.5 μA) and chronoamperometric (**b**) (E_{appl}=0.5, 0.75 and 1 V) transients of a Ag^+-selective membrane (0.35 wt% BME-321 ionophore, 70 mol % NaTFPB, 33 wt% PVC, 66 wt% DOS)

concentration of intrinsic sites (0.06 mmol/kg PVC) [48] was typically less than 1% of the mobile sites concentrations used in this study and was neglected. I_{init} is the initial current measured upon the application of the voltage (t=0), which in practice typically means the current measured at t=0.1 s. A similar equation has been derived for the time instance of the breakpoint in CP experiments [23], the only difference being that instead of the initial current (I_{init}), the applied constant current (I_{appl}) appears in the expression.

$$\tau^{1/2} = \frac{nFA\left(C_{\text{L,tot}} - \frac{k}{n}C_{\text{site}}\right)\sqrt{D_{\text{L,free}}\pi}}{2\,k\,I_{\text{appl}}} \tag{3}$$

We have assumed in these calculations that the ionophore–ion stoichiometry does not change during the polarization. It might be that close to the breakpoint this assumption is not valid and smaller stoichiometry complexes are also formed at the positively polarized side of the membrane due to the depletion of the free ionophore. However, this should affect only the curvature of the transient near the breakpoint and not the time instance of the breakpoint which is obtained by the linear extrapolation of sections on the transients before and after the breakpoint.

The constant current assumption until the breakpoint is not fulfilled in CA experiments. Therefore, although Eqs. 2 and 3 are very similar, Eq. 2 is only a good approximation while Eq. 3, which represents the constant current CP conditions, is an exact expression for $\tau^{1/2}$. Figure 2 shows CA and CP transients for BME-321-based Ag^+-selective membranes recorded in very similar current-potential regime.

From Fig. 2 it is obvious that the breakpoint can be much more easily evaluated from the CP than from the CA transients. Indeed, in the CA experiments shown in Fig. 2b the breakpoint times could not be assessed reliably as a consequence of the rapidly changing initial currents. Thus, in our experience the chronopotentiometric method is in general more "robust", i.e., it can provide reliable results for a wider range of membrane compositions, and it is less sensitive to the selected experimental conditions. The chronoamperometric method is likely to fail when the product of the membrane area and its resistance is below 80 kΩ×cm^2 and both the CA and CP methods can give erroneous results if the membrane resistance is comparable to that of the bathing solutions (data not shown). However, with practically relevant membrane compositions the latter constraint can be easily overcome.

The membrane composition is still an important criterion for the applicability of the CP and CA methods, since it was shown recently that not only the depletion of free ionophore can lead to a breakpoint in the CA and CP transients. Depending on the relative concentrations and diffusion coefficients of the free ionophore and the ion–ionophore complex, it is possible that the ion–ionophore complex concentration approaches zero first and causes a breakpoint [23].

The equation for the ion–ionophore complex breakpoint for different complex stoichiometries and multiply charged primary ions can be derived similarly to the singly charged ion case described previously [22, 23]. The differential equation describing diffusion is preserved: $\frac{\partial C_{IL_k^{n+}}}{\partial t} = D_s \frac{\partial^2 C_{IL_k^{n+}}}{\partial x^2}$, where $C_{IL_k^{n+}}$ is the concentration of the ion–ionophore complex, except, for multiply charged primary ions the effective salt diffusion coefficient is $D_s = \frac{(n+1)D_{R^-}D_{IL_k^{n+}}}{n\left(nD_{IL_k^{n+}}+D_{R^-}\right)}$ for multiply charged primary ions. In addition, the boundary conditions are different for multiply charged primary ions, becoming $\frac{I}{nF} = J_{IL_k^{n+}} = -\frac{D_s}{1-t_+}\frac{\partial C_{IL_k^{n+}}}{\partial x}\Big|_{x=\pm d}$. The transport number for cations is defined as $t_+ = \frac{nD_{IL_k^{n+}}}{nD_{IL_k^{n+}}+D_{R^-}}$ and $D_{\text{IL}_k^{n+}}$ and D_{R^-} are the diffusion coefficients of the ion–ionophore complex and lipophilic anion, respectively. Following the same steps as described previously for the case of singly charged primary ion [22, 23], the equation for the ion–ionophore breakpoint can be derived as:

$$\tau^{1/2}_{\text{IL}_k^{n+}} \approx \frac{nFC_{\text{IL}_k^{n+}}\sqrt{D_s\pi}}{2I^0\,(1-t_+)} = \frac{nFC_{\text{IL}_k^{n+}}}{2I^0}\sqrt{\frac{(n+t)\,D_{\text{IL}_k^{n+\pi}}}{n(1-t_+)}} \tag{4}$$

Therefore for complex stoichiometry and multiply charged ions the criterion for a free ionophore controlled breakpoint is given by:

$$\frac{n\,C_{\text{L,tot}}}{k\,C_{\text{site}}} - 1 < \sqrt{\frac{(n+1)D_{\text{IL}_k^{n+}}\left(n\,D_{\text{IL}_k^{n+}} + D_{\text{R}^-}\right)}{n\,D_{\text{L,free}}D_{\text{R}^-}}} \tag{5}$$

While the diffusion coefficient of the ionophores and ion–ionophore complexes can be determined rather accurately [35], the values for the diffusion coefficient of the mobile sites are inconsistent. Early studies suggested ca. five times smaller diffusion coefficients for the tetraphenylborate anion compared to the valinomycin ionophore $\left(D_{\text{TPB}^-} = 0.29\times10^{-8}\,\text{cm}^2/\text{s}\right)$ in IS membranes [49]. Since currently available tetraphenylborate derivatives do not exhibit absorption in the visible range, the only optically determined diffusion coefficient of a mobile site is for the colored lipophilic anion 2,4,6-trinitro-3-pentadecylphenol (TNPDP), for which a value of $2.34\pm0.02\times10^{-8}\text{cm}^2/\text{s}$ was reported (undissociated, protonated form) [33]. Electrochemical methods for diffusion coefficient assessment are based either on fitting the current transients

[50] $\left(D_{\mathrm{TFPB}^-} = 0.53 \times 10^{-8}\,\mathrm{cm}^2/\mathrm{s}\right)$ or fitting the concentration profiles resulting in the membrane during CP experiments $\left(D_{\mathrm{TFPB}^-} = 1.1 \pm 0.3 \times 10^{-8}\,\mathrm{cm}^2/\mathrm{s}\right)$ [22]. These methods apparently have a relatively high degree of uncertainty since it is difficult to account for the ion pair formation in the membrane. As the size of $TFPB^-$ is much larger than that of TNPDP a diffusion coefficient of 1.1×10^{-8} cm^2/s seems reasonable for $TFPB^-$. Since by increasing the D_{R^-} values the right side of the inequality in Eq. 5 decreases, this upper value of 1.1×10^{-8} cm^2/s was used for the calculations. In addition, for ionophores forming 1:1 complexes with their respective primary ion (valinomycin, BME-44, Sodium ionophore X, BME-3990) it was assumed that $D_{\mathrm{IL}_k^{n+}} = D_{\mathrm{L,free}}$. In case of ionophores forming higher stoichiometry complexes, such as BME-3033 (1:2) and ETH 5234 (1:3), $1.77 \times D_{\mathrm{IL}_k^{n+}} = D_{\mathrm{L,free}}$ and $3 \times D_{\mathrm{IL}_k^{n+}} = D_{\mathrm{L,free}}$ [35] were used in the calculations, respectively. These latter two relationships between the diffusion coefficients of ion–ionophore complexes and the respective free ionophores have been formulated based on determining the diffusion coefficients by potentiometric ion breakthrough measurements (the diffusion coefficient of BME-3033-Zn^{2+} complex was determined to be 8.7 (±1.2) × 10^{-9} cm^2/s) and chronopotentiometry, respectively.

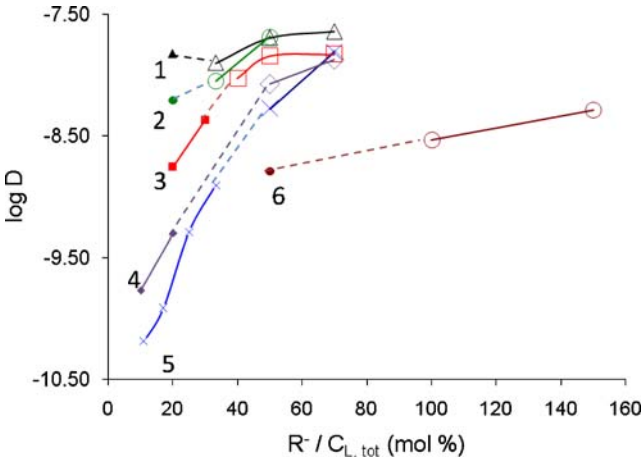

Fig. 3 The apparent concentration dependence of free ionophore diffusion coefficients in plasticized PVC membranes. The values were calculated using CA breakpoint measurements. The PVC to plasticizer ratio (33 wt% PVC, 66 wt% DOS) and the lipophilic anion concentration (1.6 mM NaTFPB) was the same in all membranes while the total ionophore content of the membranes was varied between 0.2 and 1 wt%. The different *curves* refer to membranes formulated with different ionophores: 1-valinomycin, 2-ETH 5234, 3-Na ionophore X, 4-BME-44, 5-BME-3033, and 6-BME-3990). The *large symbols* denote data where the criteria given in Eq. 5 is valid ($D_{R^-} = 1.1 \times 10^{-8}\mathrm{cm}^2/\mathrm{s}$, other conditions described in the text) while the *small filled symbols* correspond to membrane compositions for which the inequality is not valid

Figure 3 shows apparently a strong dependence of the diffusion coefficients of different ionophores on their concentration in plasticised PVC membranes. As the concentration of the free ionophores is increased in the membranes the apparent diffusion coefficients in most cases decrease dramatically. However, this strong concentration dependence mostly disappears when only those diffusion coefficients are considered which were determined in membranes whose composition fullfilled the criterion formulated in Eq. 5. Thus, the dramatic decrease in the diffusion coefficients with decreasing R^-/C_{tot} ratio is only an apparent phenomenon because when the free ionophore is in large excess the breakpoint in the CA transients is due to the depletion of the ion–ionophore complex and not that of the free ionophore. In this case Eq. 3 is certainly not valid and Eq. 4 can be in principle applied to calculate the diffusion coefficient of ion–ionophore complexes. Figure 3 also suggests that our approximation for the diffusion coefficient of the $TFPB^-$ anion is adequate since Eq 5, in which D_{R^-} (D_{TFPB^-}) is used, properly delimited the regimes of ionophore or ion–ionophore control of the breakpoint times.

To validate the chronopotentiometric technique, ETH 5294 based membranes were used at compositions where Eq. 5 is fulfilled. The diffusion coefficient of unprotonated ETH 5294 was earlier determined by a variety of optical methods with consistent results [33, 34]. Figure 4 illustrates the dependence of the diffusion coefficient of ETH 5294 ionophore on the PVC content of the IS membranes. The diffusion coefficients obtained with CA, CP and optical methods in o-NPOE plasticised PVC membranes were the same within the experimental error.

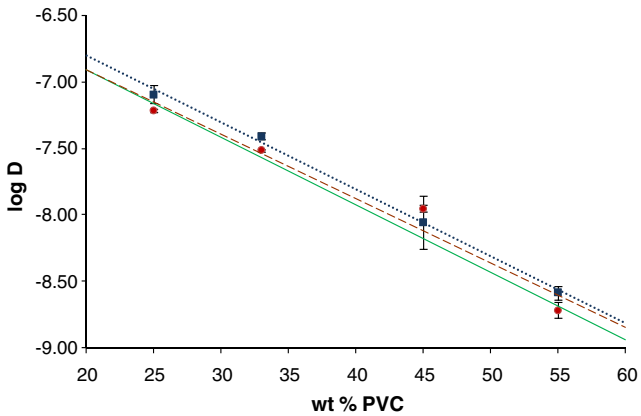

Fig. 4 Comparison of the diffusion coefficients of ETH 5294 ionophore determined with the chronoamperometric, chronopotentiometric and optical techniques in *o*-NPOE plasticized membranes of different PVC content. (—optical [$\log D = -0.051\times$ wt % PVC − 5.89] [34], - - - chronopotentiometric [$\log D = -0.049 \times$ wt % PVC − 5.93] (in 50 mM citrate buffer pH=5) and ⋯ chronoamperometric [$\log D = -0.051 \times$ wt % PVC − 5.79] (in 10^{-4} M HCl solution))

Table 2 Diffusion coefficients of different ionophores determined by CA and CP technique in DOS plasticized PVC membranes

Ion	Ionophore[a]	k	$[R^-]/C_{L,tot}$	CP		CA		CA		CA	
				D $\times 10^{-8}$ cm^2/s	RSD (%)	D $\times 10^{-8}$ cm^2/s ($I_{average}$)	RSD (%)	D $\times 10^{-8}$ cm^2/s ($I_{initial}$)	RSD (%)	D $\times 10^{-8}$ cm^2/s ($I_{breakpoint}$)	RSD (%)
K^+	Valinomycin	1	0.7	2.36	3.68	2.26	2.25	2.57	2.63	1.97	6.61
Ag^+	BME-321	1	0.7	0.96	5.16	n. d.	n. d.	n. d.	n. d.	n. d.	n. d.
K^+	BME-44	1	0.7	1.19	2.22	1.35	19.93	1.54	17.11	1.17	23.16
Na^+	Na ionophore X	1	0.7	1.46	4.41	1.48	3.63	1.71	0.11	1.27	7.70
Pb^{2+}	BME-3990	1	1.5	0.52	21.11	0.44	12.12	0.49	11.23	0.40	13.40
Zn^{2+}	BME-3033	2	0.7	1.55	0.53	1.54	1.83	1.64	2.87	1.45	1.35
Ca^{2+}	ETH5234	3	0.5	2.16	0.98	2.07	1.16	2.22	2.10	1.91	2.22

The dependence of the chronoamperometrically determined diffusion coefficients on the current value used for calculation, i.e., whether $I_{average}$, $I_{initial,}$ or $I_{breakpoint}$ is inserted in Eq. 2, is provided.
n.d. The chronoamperometric method failed to provide breakpoints
[a] Membranes with theoretically predicted optimal compositions (mol % of TFPB) were used [51]

Similarly good correlation was found for DOS plasticized membranes (data not shown). The regression lines in the log D vs. wt% PVC plots for the DOS plasticized membranes were: optical [$\log D = -0.046 \times$ wt % PVC $- 6.17$] [34], chronopotentiometry [$\log D = -0.045 \times$ wt % PVC$-$ 6.33] and chronoamperometric measurements [$\log D = -0.041 \times$ wt%PVC $- 6.37$]. Related to the diffusion coefficients calculated from CA experiments it must be noted the current values in Eq. 2 were average values, $I_{average}$, measured at $t = \tau/2$ [35]. The validity of using $I_{average}$ seems to be supported by the good agreement between chronopotentiometrically and chronoamperometrically determined diffusion coefficients as shown in Table 2 for seven ionophores. Indeed, in most cases the introduction of $I_{average}$ values in Eq. 2 provided the smallest bias in the diffusion coefficient values determined by the CA and CP method. An exception was for BME-44 and BME-3990 ionophores, for which, however, the uncertainty of those determinations was relatively high. For the other ionophores, a remarkably low bias of less than 5% was observed. The comparison of the diffusion coefficients calculated from CA and CP experiments (Table 2) was performed to evaluate the accuracy of previously reported diffusion coefficients determined by the CA method [35, 37].

Conclusion

In summary, the diffusion coefficients of the various ionophores in membranes of the same composition, i.e, the same plasticizer and PVC content, are rather similar. However, the differences are not negligible and a close to half order of magnitude difference was observed between the smallest and largest free ionophore diffusion coefficient value. Molecules with linear tails and less bulky structural units seem to have larger diffusion coefficients (ETH 5294, ETH 5234), while calixarenes have the smallest diffusion coefficients (Na ionophore X, BME-321, BME-3990). Further interpretation of the results without the exact knowledge of the structures of ionophores in the membrane matrix would become speculative. The CP method clearly succeeded in providing diffusion coefficients in plasticized PVC membranes for all the studied ionophores, which suggests that it can be a generally applicable method for the assessment of the diffusion coefficient of any neutral ionophore.

Acknowledgement This work has been supported by the Hungarian Scientific Fund (OTKA NF 69262, T46403). EL acknowledges the financial assistance of NSF # 0202207, NIH/NHLBI #1 RO1 HL079147-03 grants and the NSF Graduate Research Fellowship program. RGy acknowledges the support of the Bolyai János Fellowship.

References

1. Sokalski T, Ceresa A, Zwickl T, Pretsch E (1997) J Am Chem Soc 119:11347 doi:10.1021/ja972932h
2. Sokalski T, Zwickl T, Bakker E, Pretsch E (1999) Anal Chem 71:1204 doi:10.1021/ac980944v
3. Püntener M, Vigassy T, Baier E, Ceresa A, Pretsch E (2004) Anal Chim Acta 503:187 doi:10.1016/j.aca.2003.10.030
4. Vigassy T, Gyurcsányi RE, Pretsch E (2003) Electroanalysis 15:1270 doi:10.1002/elan.200302818
5. Bakker E, Meyerhoff ME (2000) Anal Chim Acta 416:121 doi:10.1016/S0003-2670(00)00883-7
6. Lindner E, Gyurcsányi RE, Buck RP (1999) Electroanalysis 11:695 doi:10.1002/(SICI)1521-4109(199907)11:10/11<695::AID-ELAN695>3.0.CO;2-G
7. Gyurcsányi RE, Pergel E, Nagy R, Kapui I, Lan BTT, Tóth K et al (2001) Anal Chem 73:2104 doi:10.1021/ac000922k
8. Bakker E (1997) Anal Chem 69:1061 doi:10.1021/ac960891m
9. Szigeti Z, Malon A, Vigassy T, Csokai V, Grun A, Wygladacz K et al (2006) Anal Chim Acta 572:1 doi:10.1016/j.aca.2006.05.009
10. Pergel K, Gyurcsányi RE, Tóth K, Lindner E (2001) Anal Chem 73:4249 doi:10.1021/ac010094a
11. Lindner E, Zwickl T, Bakker E, Lan BTT, Tóth K, Pretsch E (1998) Anal Chem 70:1176 doi:10.1021/ac970952w
12. Sutter J, Lindner E, Gyurcsányi RE, Pretsch E (2004) Anal Bioanal Chem 380:7 doi:10.1007/s00216-004-2737-4
13. Sutter J, Radu A, Peper S, Bakker E, Pretsch E (2004) Anal Chim Acta 523:53 doi:10.1016/j.aca.2004.07.016
14. Chumbimuni-Torres KY, Rubinova N, Radu A, Kubota LT, Bakker E (2006) Anal Chem 78:1318 doi:10.1021/ac050749y
15. Konopka A, Sokalski T, Lewenstam A, Maj-Zurawska M (2006) Electroanalysis 18:2232 doi:10.1002/elan.200603652
16. Sundfors F, Bereczki R, Bobacka J, Tóth K, Ivaska A, Gyurcsányi RE (2006) Electroanalysis 18:1372 doi:10.1002/elan.200603541
17. Rosatzin T, Holy P, Seiler K, Rusterholz B, Simon W (1992) Anal Chem 64:2029 doi:10.1021/ac00042a004
18. Dinten O, Spichiger UE, Chaniotakis N, Gehrig P, Rusterholz B, Morf WE et al (1991) Anal Chem 63:596 doi:10.1021/ac00006a009
19. Makarychev-Mikhailov S, Shvarev A, Bakker E (2006) Anal Chem 78:2744 doi:10.1021/ac052211y
20. Gemene KL, Shvarev A, Bakker E (2007) Anal Chim Acta 583:190 doi:10.1016/j.aca.2006.09.042
21. Bhakthavatsalam V, Shvarev A, Bakker E (2006) Analyst (Lond) 131:895 doi:10.1039/b602906j
22. Zook JM, Buck RP, Langmaier J, Lindner E (2008) J Phys Chem B 112:2008 doi:10.1021/jp074612i
23. Zook J, Buck RP, Gyurcsányi RE, Lindner E (2008) Electroanalysis 20:259 doi:10.1002/elan.200704052
24. Gyurcsányi RE, Lindner E (2006) Cytometry A 69A:792 doi:10.1002/cyto.a.20276
25. Gyurcsányi RE, Lindner E (2005) Anal Chem 77:2132 doi:10.1021/ac048445j
26. Lindner E, Gyurcsányi RE, Pendley BD (2001) Pure Appl Chem 73:17 doi:10.1351/pac200173010017
27. Schneider B, Zwickl T, Federer B, Pretsch E, Lindner E (1996) Anal Chem 68:4342 doi:10.1021/ac9604245
28. Peshkova MA, Korobeynikov AI, Mikhelson KN (2008) Electrochim Acta 53:5819 doi:10.1016/j.electacta.2008.03.030
29. Wang H, Sun L, Armstrong RD (1996) Electrochim Acta 41:1491 doi:10.1016/0013-4686(95)00400-9
30. Mokrov SB, Malev VV, Stefanova OK (1990) Sov Electrochem 26:973
31. Püntener M, Fibbioli M, Bakker E, Pretsch E (2002) Electroanalysis 14:1329 doi:10.1002/1521-4109(200211)14:19/20<1329::AID-ELAN1329>3.0.CO;2-V
32. Crank J (1975) The mathematics of diffusion. Clarendon, Oxford
33. Moczár I, Gyurcsányi RE, Huszthy P, Jágerszki G, Tóth K, Lindner E (2006) Electroanalysis 18:1396 doi:10.1002/elan.200603551
34. Long R, Bakker E (2004) Anal Chim Acta 511:91 doi:10.1016/j.aca.2004.01.028
35. Bodor S, Zook J, Lindner E, Tóth K, Gyurcsányi ER (2008) Analyst (Lond) 133:635 doi:10.1039/b718110h
36. Pendley BD, Lindner E (1999) Anal Chem 71:3673 doi:10.1021/ac990137b
37. Pendley BD, Gyurcsányi RE, Buck RP, Lindner E (2001) Anal Chem 73:4599 doi:10.1021/ac010007e
38. Sokalski T, Ceresa A, Fibbioli M, Zwickl T, Bakker E, Pretsch E (1999) Anal Chem 71:1210 doi:10.1021/ac9809332
39. Gehrig P, Rusterholz B, Simon W (1989) Chimia (Aarau) 43:377
40. Lindner E, Tóth K, Jeney J, Horváth M, Pungor E, Bitter I et al (1990) Mikrochim Acta 1:157 doi:10.1007/BF01244839
41. Cadogan AM, Diamond D, Smyth MR, Deasy M, McKervey MA, Harris SJ (1989) Analyst (Lond) 114:1551 doi:10.1039/an9891401551
42. Csokai V, Bitter I (2004) Supramol Chem 16:611 doi:10.1080/10610270412331318818
43. Lindner E, Horváth M, Tóth K, Pungor E, Bitter I, Ágai B et al (1992) Anal Lett 25:453
44. Thoma AP, Viviani-Nauer A, Arvanitis S, Morf WE, Simon W (1977) Anal Chem 49:1567 doi:10.1021/ac50019a027
45. Iglehart ML, Buck RP, Horvai G, Pungor E (1988) Anal Chem 60:1018 doi:10.1021/ac00161a014
46. Morf WE, Wuhrmann P, Simon W (1976) Anal Chem 48:1031 doi:10.1021/ac60371a029
47. Lev AA, Malev VV, Osipov VV (1973) In: Eisenman G (ed) Lipid bilayers and antibiotics. M. Dekker, New York
48. Gyurcsányi RE, Lindner E (2002) Anal Chem 74:4060 doi:10.1021/ac020120k
49. Armstrong RD, Todd M (1987) Electrochimica Actab 32:155
50. Nahir TM, Buck RP (1993) J Phys Chem 97:12363 doi:10.1021/j100149a043
51. Eugster R, Gehrig PM, Morf WE, Spichiger UE, Simon W (1991) Anal Chem 63:2285 doi:10.1021/ac00020a017